Tectonophysics 864 (2023) 229985

Contents lists available at ScienceDirect

Tectonophysics

journal homepage: www.elsevier.com/locate/tecto

Late Holocene tectonics inferred from emerged shoreline features in Higashi-Izu monogenetic volcano field, Central Japan

Masanobu Shishikura [a,*], Yuichi Namegaya [a], Hiroyuki Kaneko [b], Masato Koyama [c]

[a] Geological Survey of Japan, National Institute of Advanced Industrial Science and Technology, Site7 1-1-1 Higashi, Tsukuba 305-8567, Japan
[b] Ito City Education Board, 2-1-1 Ohara, Ito 414-8555, Japan
[c] Center for Integrated Research and Education of Natural Hazards, Shizuoka University, 836 Oya, Suruga-ku, Shizuoka 422-8529, Japan

ARTICLE INFO

Keywords:
Higashi-Izu monogenetic volcano field
Volcano-tectonics
Earthquake swarm
Uplift
Emerged sessile assemblage

ABSTRACT

Emerged shoreline features such as morphology, stratigraphy, and fossil assemblages are useful to reconstruct the history of vertical crustal movement in coastal areas. In particular, resolving the history of individual tectonic events can help understand regional seismo- and volcano-tectonic processes. In the eastern coast of the Izu Peninsula, central Japan, multiple levels of emerged shoreline features formed as a result of repeated uplift caused by the activity of Higashi-Izu monogenetic volcano field or related seismo-tectonic processes during the Late Holocene. To clarify the history of uplift events and the mechanism of regional tectonics, we surveyed these features with a focus on fossil sessile assemblages. Based on an analysis of their height and age, three zones associated with intermittent emergence events, denoted Zone 1 (1.05-m uplift in 595–715 CE), Zone 2 (1.33-m uplift in 1356–1666 CE), and Zone 3 (0.82-m uplift after 1830 CE), were identified. The interval between events was 400–800 years. Zone 3 can be regarded to have emerged via a stepwise but gradual uplift that lasted 130 years. This movement was caused by geodetically observed volcanic crustal deformation with earthquake swarms. We infer that zones 1 and 2 were uplifted by similar intervals of volcanic deformation, but cannot discard coseismic contributions from offshore faults as a possible explanation. The timing of these emergence events coincides with periods of both increased volcanic and seismic activities in the vicinity, suggesting that they are interrelated. Based on the height and age of the additional older assemblage denoted Zone 0 overlying Zone 1 and those of the post-glacial transgressive deposits in the adjacent areas, we suggest that the crustal uplift of the Izu Peninsula was initiated around 3000 years ago, which coincides with the largest eruption of Kawagodaira volcano. Therefore, volcanic activity is an important factor governing coastal uplift in this region.

1. Introduction

To understand the interaction between the volcanotectonic activity and surrounding tectonic settings, it is important to investigate crustal deformation related to subsurface magma movement. Geophysical surveys such as seismic, geomagnetic, and geodetic observations are generally used for this purpose, but it is also necessary to obtain historical and geological data in order to evaluate long-term activity over the period prior to starting instrumental observation (e.g., Gudmundsson, 2020; Acocella, 2021). However, while common geological methods such as stratigraphic and material analyses of volcanic deposits can reconstruct the eruption history, they are unsuitable for detecting volcanotectonic movement quantitatively. Therefore, we here focused on traces of past shorelines along the coast of active volcanic areas.

The morphology, stratigraphy, and fossil assemblages found at coastlines often comprise a record of vertical deformation. For example, in seismotectonically active coastal areas, evidence of repeated uplift events caused by large earthquakes is commonly found in the form of emerged shoreline morphology and emerged sessile assemblages. The height distribution and age of emerged shorelines have long been used to reconstruct earthquake histories and relative sea level (RSL) change (e.g., Pirazzoli, 1996; Nelson, 2013; Kelsey, 2015). Some studies focusing on the relationship between volcanism and Pleistocene to Holocene RSL changes have also been conducted in volcanic areas such as Iwo Jima (Kaizuka, 1992), the area around Mount Etna (details described later), Nisyros Island in the Aegean Sea (Stiros et al., 2005), Sabatini caldera near Rome (Marra et al., 2019), and the Campi Flegrei caldera near Napoli (Todesco et al., 2013; Marturano et al., 2018; Costa

* Corresponding author.
E-mail address: m.shishikura@aist.go.jp (M. Shishikura).

https://doi.org/10.1016/j.tecto.2023.229985
Received 25 March 2022; Received in revised form 28 June 2023; Accepted 29 June 2023
Available online 13 July 2023

et al., 2022). Since these sites, except for the area around Etna volcano, have no particular large-scale tectonic structures and are limited to areas in very close proximity to the volcano, detected crustal deformation can be simply interpreted as uplift and subsidence mainly due to magmatic activity, and thus the relationship with the surrounding tectonic setting has been little discussed.

The area around Mt. Etna is considered to be affected by the interaction between the European and African plates, and the eastern flank of Mt. Etna expands into the Ionian Sea to the southeast due to volcanic activity. Many studies have been conducted to investigate the actual state of long-term crustal deformation from Pleistocene marine deposits (Di Stefano and Branca, 2002; Catalano et al., 2004; Antonioli et al., 2006; Ristuccia et al., 2013), and from Holocene paleoshoreline features (Firth et al., 1996; Rust and Kershaw, 2000). However, they have been interpreted rather as the result of tectonic variations, and a cause related to volcanism was not identified. This region is too complex to make a clear distinction between volcanic activity and tectonic variations. Therefore, to evaluate the long-term volcanotectonic history due to subsurface magma movement and interaction with seismotectonics, it is better to study the separation of volcanism and tectonic deformation in areas with simpler crustal structures, where both volcanism and tectonic deformation are active, their history is well documented, and recent crustal deformation is well monitored by dense instrumental observation networks. Especially in studies using emerged shoreline features, regional RSL histories should also be well-known from other surveys.

The northern extreme of the Izu-Bonin-Mariana (IBM) Arc, located in central Japan, is one of the most suitable areas for such a study because it is located in the collision zone with the Honshu Islands, where crustal deformation is active, and the history of volcanism, crustal structure, and RSL has been well studied. Along the eastern coast of the Izu Peninsula, we found multiple levels of emerged shoreline features mainly composed of fossil sessile assemblages. This area, called the Higashi-Izu monogenetic volcano field, is very volcanically and seismically active (Aramaki and Hamuro, 1977). Previous geological studies have revealed volcanic activity over the last 150,000 years (Hayakawa and Koyama, 1992; Koyama et al., 1995), and reconstructed the history of inland active faults and subduction megathrust earthquakes in the surrounding area over the mid-late Holocene (The Tanna Fault Trenching Research Group, 1983; Kondo et al., 2003; Shishikura, 2014; Komori et al., 2017). Crustal deformation due to volcanic activity, intraplate faulting, and subducting plate motion in the period before the 19th century is quantitatively unknown, even though relatively dense instrumental observation data exist for the past hundred years for this area. Therefore, we analyzed the height distribution and age of emerged shorelines discovered as part of this investigation and attempted to

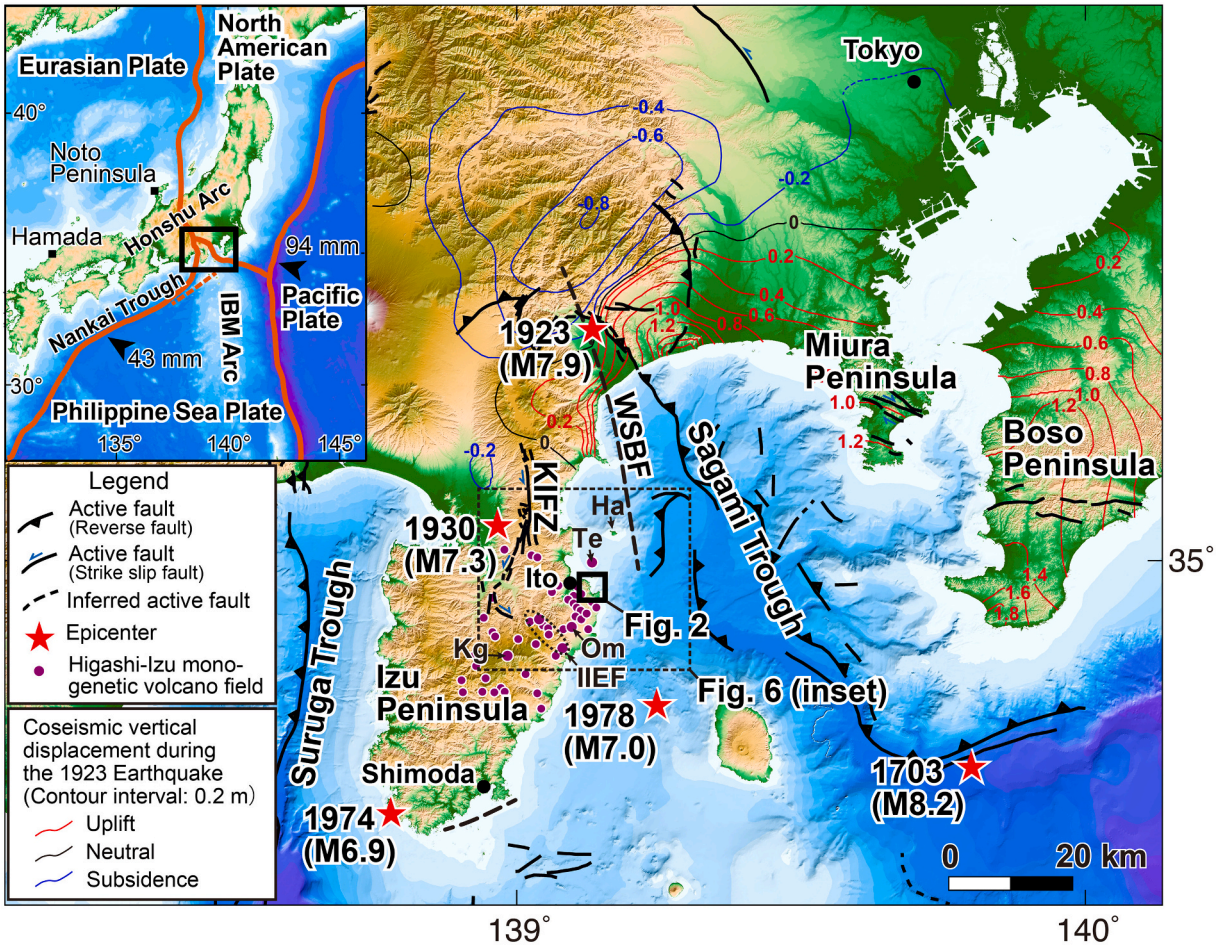

Fig. 1. Tectonic setting around the Izu Peninsula and the location of the survey area. IBM Arc: Izu-Bonin-Mariana Arc. KIFZ: Kita-Izu Fault Zone. WSBF: West Sagami Bay Fault. IIEF: Iwanoyama-Ioyama Eruptive Fissure. Kg: Kawagodaira Volcano. Om: Omuroyama Volcano. Te: Teishi Knoll. Ha: Hatsushima Island. Plate motion in the inset is after Bird (2003). Traces of active faults are after Headquarters for Earthquake Research Promotion, Earthquake Research Committee (2015) in onshore region, after Okamura et al. (1999) in offshore region around Izu Peninsula, and after Research Group for Active Fault of Japan (Eds.), 1991 in other offshore regions. Faulting sense of inferred active faults is not specified. Epicenters are after Usami et al. (2013). Distribution of volcanoes in the Higashi-Izu monogenetic volcano field is after Koyama et al. (1995). Contours of coseismic vertical displacement during the 1923 Taisho Kanto earthquake are compiled from Land Survey Department (1926) and Miyabe (1931).

reconstruct the history of uplift in the Higashi-Izu monogenetic volcano field with consideration of the causes of the emergence events. This information can contribute to our understanding of geodynamics in a volcanic arc and highlight the usefulness of emerged shoreline feature investigations in the long-term evaluation of volcanic activity. Furthermore, the results are expected to be useful for volcano-related and seismicity-related disaster prevention near metropolitan regions of Japan.

2. Setting

The Izu Peninsula, located at the northern extreme of the IBM Volcanic Arc, formed approximately 1 million years ago due to the collision of an island on the north-moving Philippine Sea Plate with the Honshu Arc (Sugimura, 1972; Matsuda, 1978) (Fig. 1). The Philippine Sea Plate has continued to move in a northwesterly direction after the collision and is being subducted underneath the North American Plate along the Sagami Trough to the east of the peninsula and underneath the Eurasian Plate along the Suruga Trough to the west of the peninsula, leading to seismic events. The study area faces the Sagami Trough, where two historically large earthquakes, namely the 1703 Genroku Kanto earthquake (M8.2) and the 1923 Taisho Kanto earthquake (M7.9), are well-known interplate megathrust events (Fig. 1). Although fault mechanisms are unknown, older events, such as those in 878, 1293, and 1433 or 1495, have also been proposed based on historical records and are partly supported by geological evidence (Shimazaki et al., 2011; Kaneko, 2012; Ishibashi, 2020). Investigations of marine terraces and tsunami deposits along the coasts of the Boso and Miura Peninsulas have revealed a history of repeated megathrust earthquakes with a mean interval of 400 years since the middle Holocene (Shishikura, 2003, 2014). Abundant historical records for the Nankai Trough, which extends southwestward from the Suruga Trough, indicate a history of repeated megathrust earthquakes over the past 1300 years every 100 to 200 years (Usami et al., 2013). The Kita-Izu fault zone (KIFZ), which contains inland strike slip active faults with a left-lateral sense located in the northern part of the peninsula, is believed to have ruptured at intervals of 460 to 1600 years and was the source of the 1930 Kita-Izu earthquake (M7.3) (The Tanna Fault Trenching Research Group, 1983; Kondo et al., 2003). Offshore active faults have also been detected around the Izu Peninsula (Okamura et al., 1999). Although far from the study area, uplift traces in Shimoda associated with offshore fault activity off the southernmost part of the peninsula were identified and linked to four events in the past 3000 years (Fukutomi, 1935; Kitamura et al., 2015).

The collision of the Izu Peninsula due to the northward motion of the Philippine Sea Plate has induced magma intrusion and produced a series of craters from a monogenetic volcano (Higashi-Izu monogenetic volcano group) striking in the northwest-southeast direction on the eastern side of the peninsula (Aramaki and Hamuro, 1977; Koyama and Umino, 1991). Although the geology provides an eruption record going back approximately 150,000 years, in the Holocene, the first major eruption was the Omuroyama eruption around 2000 BCE, followed by the Kawagodaira eruption, the largest eruption in the last 100,000 years, in 1210–1187 BCE (Hayakawa and Koyama, 1992; Koyama et al., 1995; Tani et al., 2013). This was followed by the Iwanoyama-Ioyama eruptive fissure around 800–700 BCE. After these activities, both the geological and historical records indicate that no major eruption occurred except for a small phreatomagmatic explosion of the Teishi Knoll off the coast of Ito in 1989. Seismic observation data for the last hundred years show that there were two active phases of frequent earthquake swarm events accompanied by subsurface magma intrusion in this area, including the offshore area. The first phase was recorded in 1930 (Nasu et al., 1931). In the second phase, from 1978 to 2011, the area experienced 49 earthquake swarms (Japan Meteorological Agency, 2014). Related to these activities, gradual uplift was geodetically observed from leveling and tide gauge data (Geospatial Information Authority of Japan, 2016). Before the first phase of the earthquake swarm in 1930, historical records suggest the occurrence of similar earthquakes for at least two periods, namely 1816 to 1817 and 1868 or 1870, at an interval of 50–60 years (Koyama, 1999; Table S1).

3. Methods

We conducted a field survey of the rocky coast in the vicinity of Ito, the northeastern part of the Izu Peninsula, in which we first confirmed the distribution of emerged paleoshorelines, and then identified fossils of littoral sessile assemblages. In terms of emerged shoreline morphology, we surveyed the surface of wave-cut benches and wave-cut notches, which are primarily formed in intertidal zones. We also observed the distribution of sessile assemblages, noting the height of their upper and lower boundaries as well as their species composition, and collected samples for ^{14}C dating. Elevation measurements using a GS10 Virtual Reference Station (Leica Geosystems AG) are given with respect to Tokyo Peil (T.P.), which is the mean sea level of Tokyo Bay. To clarify the relationship between the elevations of emerged shoreline features and present-day shoreline indicators, we performed a similar investigation and measurement of the present shoreline morphology and sessile assemblages as modern analogs. The relative height between the paleoshorelines of multiple levels reconstructed from these data indicates the amount of RSL change. Although this method introduces some errors in the identification and measurement of paleoshoreline indicators, the uncertainty of RSL in this study is calculated to be relatively small at 0.08 m based on the formulas of Rovere et al. (2016). We thus use the measured data directly to discuss RSL change.

Radiocarbon dating of collected samples was performed by Beta Analytic Inc. Measured ages were calibrated using the OxCal program version 4.4 (Bronk Ramsey, 2009) with the Marine20 curve (Heaton et al., 2020). Reported values for the local variation (ΔR) of the marine reservoir effect in areas near the study site ranged from positive values of +109 yr in the southern part of the Izu Peninsula (Yoneda et al., 2000) and + 83 ± 33 yr on the Miura Peninsula (Shishikura et al., 2007) to a negative value of −24 ± 13 yr in the southern part of the Boso Peninsula (Shishikura, 2019), illustrating the high variability within this relatively small area. In this study, we thus describe ages based on the global average $\Delta R = 0$. Values reported for nearby areas are also discussed.

4. Results

4.1. Species of identified organism

Multiple emerged paleoshorelines at elevations below ~4 m T.P. were observed along the coast southeast of central Ito City. At five sites (Locs. 1–5), we found emerged sessile assemblages (Figs. 2, 3). Locs. 1–4 are close to each other, roughly within 0.8 km, but Loc. 5 is at a distance of 1.4 km to the southeast of Loc. 4. At Locs. 2–4, sessile assemblages were attached to the walls of sea caves (Figs. 3, S2, S4, S5). At Locs. 1 and 5, they were attached above an emerged wave-cut bench and to an emerged wave-cut notch (Figs. S1, S6). The dominant organisms comprising these sessile assemblages included *Chthamalus challengeri* Hoek (Cc) and other barnacles as well as the polychaete worm *Pomatoleios kraussii* (Pk) and other tube worms (Fig. S7), in rare cases interspersed with bivalves such as *Barbatia (Savignyarca) virescens*. In this study, we extracted primarily Pk for ^{14}C dating. The habitat of Pk is limited to low- and mid-intertidal zones and its upper level corresponds to around mean sea level. Thus it is an extremely useful index for reconstructing paleo-sea levels (Kayanne et al., 1987).

4.2. Elevations of present-day organisms

Present-day Pk assemblages in this area were observed at elevations ranging from −0.60 to +0.30 m T.P. (vertical span of 0.90 m), with the upper level varying locally between +0.15 and + 0.30 m T.P. (Fig. 4).

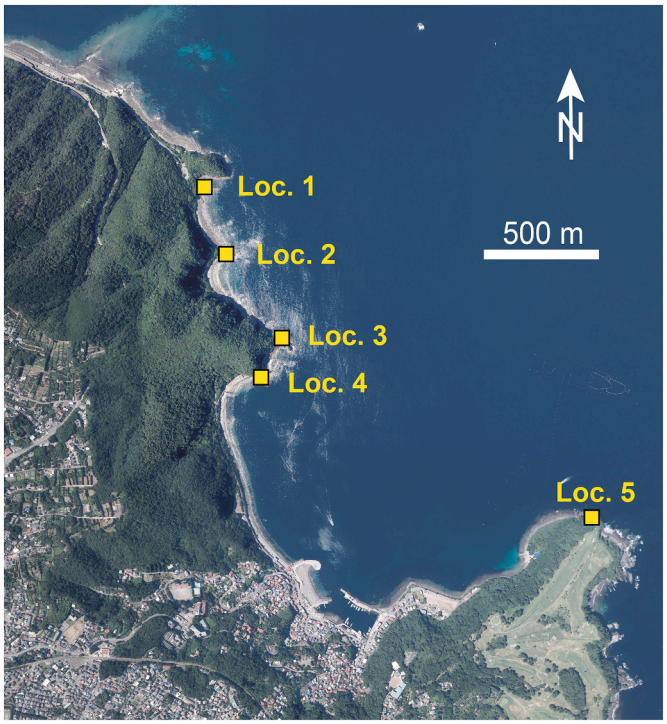

Fig. 2. Survey points in the study area. Location is shown in Fig. 1. The base map is an aerial photograph published by the Geospatial Authority of Japan.

Some Cc samples were also subjected to ^{14}C dating. It is known that the Cc habitat overlaps that of Pk in the intertidal zone but that its range extends higher than that for Pk into the high-intertidal zone and, in some cases, even above the high tide level (Mori, 1986). Kitamura et al. (2014) reported that the Cc habitat is dominant up to +0.60 m T.P. and rarely reaches +0.70 m T.P. in the southernmost part of the Izu Peninsula. Although we were unable to determine the vertical distribution of present-day Cc assemblages in this area, considering these previous reports and the mean high tide elevation in this area (approximately +0.70 m T.P.) observed at the Ito tide gauge station, we can assume that Cc is distributed to a maximum height of at least +0.70 m T.P. The lower range of Cc is probably around mean low tide elevation.

4.3. Elevations and ages of emerged organism

Based on the elevations of the corresponding emerged shoreline morphology and the ^{14}C ages of component organisms, we classified the assemblages found at elevations of 3.50 m T.P. or lower into three zones (Zones 1 to 3) in descending order (Fig. 3 and Table 1). Although the vertical distribution of the assemblages among the zones is slightly scattered due to differences in local habitat or the effect of denudation, the zones were defined by assemblages consisting primarily of Pk, whose vertical spans are 0.95 m in Zone 1, 1.20 m in Zone 2, and 0.82 m in Zone 3, respectively. For example, at Loc. 2, sessile assemblages were found attached to the walls of two notches at different elevations, namely Zones 1 and 2, within the same sea cave (Figs. 3 and S2). Zone 3 assemblages were distributed at elevations near the current sea level (Figs. 3, S3, S5). Above Zone 1 at Loc. 2, emerged sessile assemblages were distributed up to an elevation of 4.20 m T.P., but this was not defined as a zone due to the absence of Pk (Fig. S2). We thus named this assemblage Zone 0.

Zone 1 assemblages were identified at two sites (Locs. 2 and 3). They were distributed at elevations between 2.55 and 3.50 m T.P. at Loc. 2 and between 2.85 and 3.45 m T.P. at Loc. 3 (Fig. 4). At Loc. 2, the assemblages were continuously distributed and covered the whole of the emerged wave-cut notch (Fig. S2). The total vertical span in Zone 1 was 0.95 m, which is almost the same as that of the present-day Pk assemblages. Four samples collected at elevations of 3.40, 2.93 (two samples), and 2.69 m T.P. were ^{14}C dated to between 480 and 886 CE. Above Zone 1 at Loc. 2, Zone 0 consisting entirely of Cc was observed at an elevation of 3.50 to 4.20 m T.P. Given that the habitat of present-day Cc extends $\geq$ +0.50 m above the upper limit of Pk, this may possibly be an upward extension of Zone 1. However, samples collected at an elevation of 3.59 m T.P. were ^{14}C dated to between 1265 and 926 BCE, which is substantially earlier than the ages obtained for the underlying assemblages. Based on these observations, we consider the upper Cc assemblage to represent an older sessile assemblage that is different from those found in Zone 1.

Zone 2 assemblages were identified at all sites. Their height distribution was between 1.25 and 2.45 m T.P., giving a wider vertical span than those of the other zones (Fig. 4). At Loc. 1, the assemblages were distributed in the lowest position in Zone 2 (elevation of 1.25–1.50 m T.P.), and two obtained samples were ^{14}C dated to between 1440 and 1730 CE. The assemblages at Locs. 2–4 were in the middle to high positions in Zone 2 (elevations of 1.59–2.30 m T.P. at Loc. 2, 1.65–2.45 m T.P. at Loc. 3, and 1.64–2.04 m T.P. at Loc. 4). Five samples collected at these sites were ^{14}C dated to between 1272 and 1612 CE; this age range partially overlaps that of the samples at Loc. 1 but is slightly older. Based on the height and age of the assemblages, Zone 2 can be sub-divided into an upper section (Locs. 2–4) and a lower section (Loc. 1). The assemblage at Loc. 5 was at an elevation of 1.40–1.50 m T.P., which appears to be consistent with the lower section, but the obtained sample was dated to be older (1279–1488 CE), which is approximately the same age range

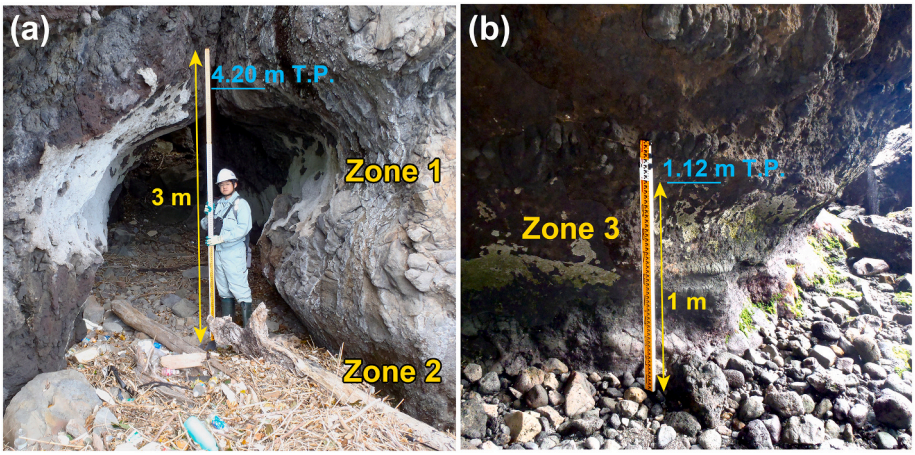

Fig. 3. Photographs of traces of emerged shorelines. Photographs taken at (a) Loc. 2 and (b) Loc. 4.

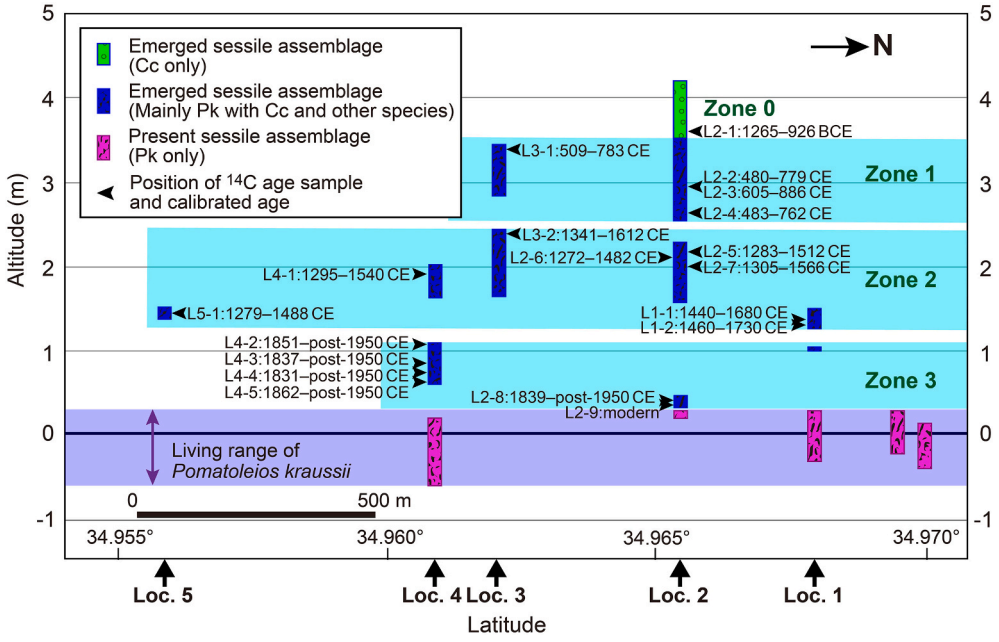

Fig. 4. Height distribution and ^{14}C ages of emerged shoreline features projected along the coast in N-S direction.

Table 1
^{14}C dating results.

Location		Sample no.	Zone	Altitude (m)	Material	Species	Conventional age	δ13C	Calendar age (ΔR = 0)	Lab. Code
Loc.1	34°58′4.54″N 139° 7′39.03″E	L1–1	2	1.36	Marine shell	*Pomatoleios kraussii*	940 ± 30	0.8	1440–1680 CE	Beta-454466
		L1–2	2	1.29	Marine shell	*Pomatoleios kraussii*	890 ± 30	1.9	1460–1730 CE	Beta-454467
Loc.2	34°57′55.69″N 139° 7′42.04″E	L2–1	0	3.59	Marine shell	*Chthamalus* sp.	3370 ± 30	0.7	1265–926 BCE	Beta-326387
		L2–2	1	2.93	Marine shell	*Chthamalus* sp.	1920 ± 40	−0.4	480–779 CE	Beta-259878
		L2–3	1	2.93	Marine shell	*Pomatoleios kraussii*	1820 ± 40	−2.6	605–886 CE	Beta-259879
		L2–4	1	2.69	Marine shell	*Pomatoleios kraussii*	1930 ± 30	−5.8	483–762 CE	Beta-326388
		L2–5	2	2.15	Marine shell	*Pomatoleios kraussii*	1130 ± 40	0.4	1283–1512 CE	Beta-259881
		L2–6	2	2.14	Marine shell	*Chthamalus* sp.	1160 ± 30	−1.9	1272–1482 CE	Beta-326389
		L2–7	2	2.05	Marine shell	*Pomatoleios kraussii*	1080 ± 40	0.2	1305–1566 CE	Beta-259880
		L2–8	3	0.37	Marine shell	*Pomatoleios kraussii*	420 ± 30	0.6	1839– post-1950 CE	Beta-454468
		L2–9	3	0.33	Marine shell	*Pomatoleios kraussii*	–	–	Modern	Beta-454469
Loc.3	34°57′43.66″N 139° 7′51.04″E	L3–1	1	3.40	Marine shell	*Pomatoleios kraussii*	1910 ± 30	0.4	509–783 CE	Beta-326385
		L3–2	2	2.40	Marine shell	*Pomatoleios kraussii*	1040 ± 30	−0.2	1341–1612 CE	Beta-326386
Loc.4	34°57′39.44″N 139° 7′47.83″E	L4–1	2	1.94	Marine shell	*Pomatoleios kraussii*	1100 ± 40	2.2	1295–1540 CE	Beta-259883
		L4–2	3	1.12	Marine shell	*Pomatoleios kraussii*	350 ± 30	0.3	1851–post-1950 CE	Beta-326381
		L4–3	3	0.84	Marine shell	*Pomatoleios kraussii*	400 ± 40	0.5	1837– post-1950 CE	Beta-259882
		L4–4	3	0.72	Marine shell	*Pomatoleios kraussii*	460 ± 30	−0.5	1831– post-1950 CE	Beta-326382
		L4–5	3	0.62	Marine shell	*Pomatoleios kraussii*	260 ± 30	−0.6	1862– post-1950 CE	Beta-326383
Loc.5	34°57′21.06″N 139°08′38.77″E	L5–1	2	1.43	Marine shell	*Pomatoleios kraussii*	1150 ± 30	1.1	1279–1488 CE	Beta-535935

as that at Locs. 2–4 in the upper section.

Zone 3 assemblages were identified at three sites (Loc. 1, 3, and 4). They were distributed at elevations between 0.30 and 1.12 m T.P. At Loc. 1, we found a small assemblage patch composed of Pk at an elevation of 1.00–1.05 m T.P. but no ^{14}C age sample was obtained (Fig. S1). The assemblage at Loc. 2 was observed at an elevation of 0.30–0.45 m T.P. in the lower position of Zone 3 (Fig. S3). The two samples obtained from this assemblage were ^{14}C dated to 1839 to Post 1950 CE in the upper part and modern in the lower part. The assemblage at Loc. 4 was almost continuously distributed from 0.62 to 1.12 m T.P. in elevation (Figs. 3, S5). Four samples collected from the top to bottom of the assemblage were all dated to after 1830 CE.

5. Discussion

5.1. Age of emergence events and amount of RSL change

Fig. 5 shows the spatiotemporal distribution of the age and elevation of the emerged sessile assemblages found in this study. This distribution allows us to determine the timing of emergence events and the amount of change in the RSL.

The vertical span of Zone 1 (0.95 m) almost matches that of the present-day Pk assemblages (0.90 m), and the ^{14}C ages of the four samples collected from the upper and lower sections of the zone were found to be concentrated in the range of 480 to 886 CE. These characteristics indicate that all of Zone 1 emerged in a relatively short time. If we assume that the four samples are of the same age, the emergence, as estimated using the Combine function of the OxCal program, occurred between 595 and 715 CE. The amount of RSL fall is estimated to have been at least 1.05 m based on the difference in the elevation of the upper

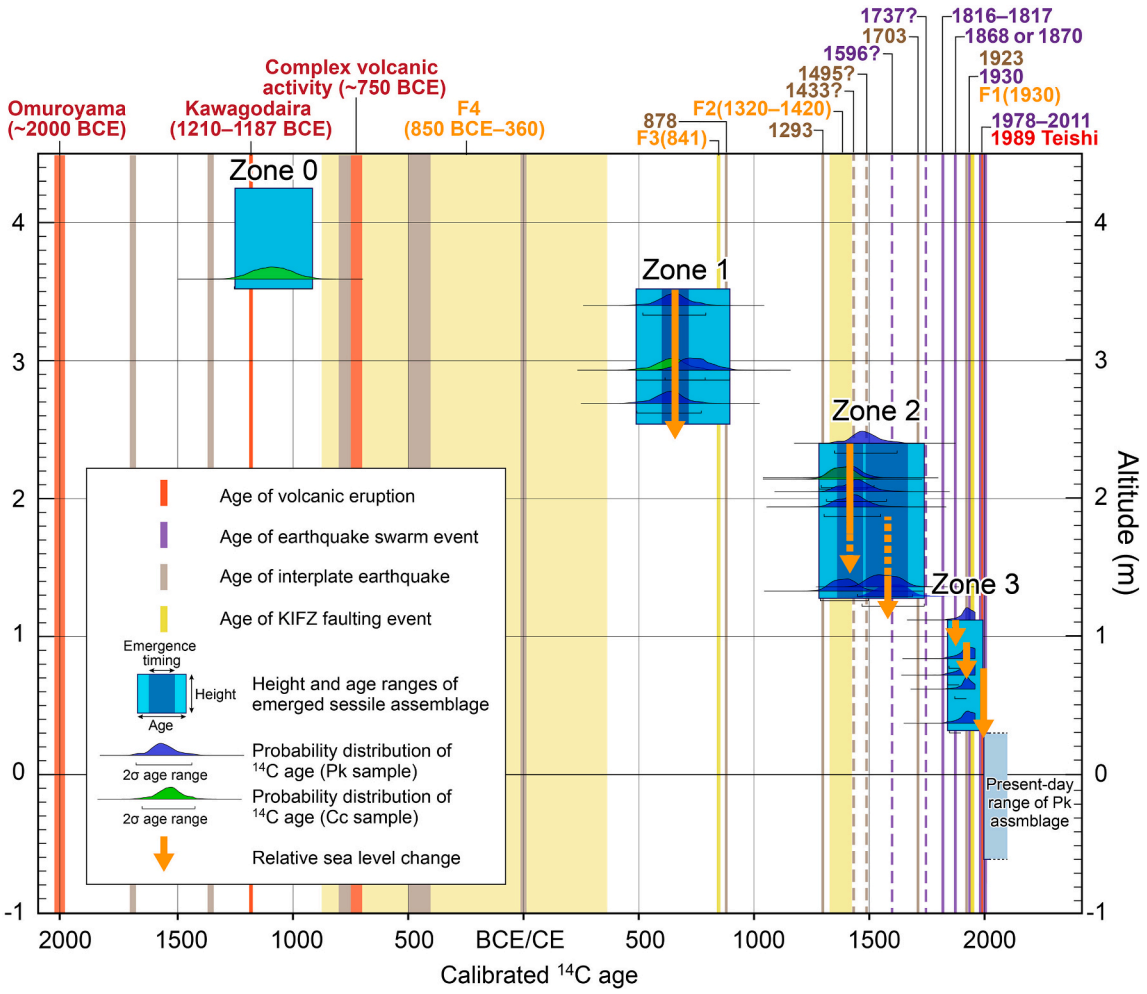

Fig. 5. Spatiotemporal diagram of emergence events with ^{14}C dating data, and timings of volcanic eruptions, earthquake swarm events, interplate earthquakes along the Sagami Trough, and faulting events of KIFZ. Age of volcanic eruption is based on the database of Quaternary volcanoes of Japan (https://gbank.gsj.jp/volcano/Quat_Vol/index_e.html). Age of earthquake swarm is after Koyama (1999). Age of interplate earthquake along the Sagami Trough is compiled from Shishikura (2014), Ishibashi (2020), and Komori et al. (2021). Age of KIFZ faulting event is after Kondo et al. (2003).

limits of the Pk assemblage between Zone 1 (3.50 m T.P.) and Zone 2 (2.45 m T.P.).

Zone 0 comprises only Cc and is found above Zone 1 at Loc. 2 at an elevation of 3.50–4.20 m T.P. It was dated to between 1265 and 926 BCE, and likely represents the oldest assemblage that emerged around 3000 years ago in this area. The amount of RSL fall is difficult to estimate precisely given the uncertainty regarding the elevation of the counterpart of the Cc assemblage in Zone 1. Nevertheless, it can be regarded that the net amount does not exceed the vertical span of this assemblage (0.70 m).

The vertical span of Zone 2 (1.20 m) is 0.30 m greater than that of the present-day Pk assemblages (0.90 m). In addition, the estimated age range of the eight samples (1272–1730 CE) is relatively wide, with the two samples in the lower section obtained at Loc. 1 tending to be younger than the five samples in the upper section obtained at Locs. 2–4. The assemblage at Loc. 5, which is located at a distance from other sampling sites, probably belongs to the upper section due to its relatively old ^{14}C age despite its lower elevation. This contradiction is considered to be due to local differences in vertical crustal movement. Therefore, we exclude the sample at Loc. 5 from the discussion here. The observation results suggest that Zone 2 comprises overlapping assemblages from two separate emergence events. Accordingly, we estimated the emergence timing using the Combine function for the five samples from the upper section and the two samples from the lower section. The upper and lower sections were dated to 1356–1470 CE and 1482–1666 CE, respectively. Although the gap between the two age ranges is 12 years at minimum and 310 years at maximum, the mode of the probability distribution is 1425 CE for the upper section and 1570 CE for the lower section, for a time gap of 145 years. As such, it is possible that Zone 2 emerged in a stepwise process over 100–200 years, starting with the upper section and followed later by the lower section. A comparison of the upper limit of the elevations of Zones 2 and 3 indicates that the total amount of RSL fall resulting from the emergence of Zone 2 in its entirety was at least 1.33 m, but this represents the total amount due to two emergence events via a stepwise process. Accurate estimation of the individual amount of RSL fall associated with each event is difficult because no reference level can be detected among the assemblages. However, the fact that the vertical span of Zone 2 is 0.30 m greater than that of the present-day Pk assemblages indicates that the amount of RSL fall from the upper section to the lower section is at least 0.30 m.

The vertical span of Zone 3 (0.82 m) almost matches that of the present-day Pk assemblages (0.90 m), but there is a possibility that the assemblages near the lower limit of the zone are mixed in with the present-day assemblages. The samples subjected to ^{14}C dating all comprised Pk, with six samples dated to 1830 CE or later and one sample dated as being modern. This suggests that the assemblages are associated with an emergence event that occurred within the past 200 years. The amount of RSL fall resulting from the emergence of Zone 3 is

estimated to be at least 0.82 m based on a comparison of the upper limits of the fossil Pk and present-day Pk assemblages.

It can be concluded from the above results that the emerged sessile assemblages distributed in three zones in the study area resulted mainly from three RSL falls that ranged in magnitude from 0.82 to 1.33 m. For these emergence events, the recurrence interval is about 800 years between Zone 1 and 2, and about 400 years between Zone 2 and 3. The emergence of Zone 0, which is the last event prior to the emergence of Zone 1, occurred approximately 3000 years ago with a vertical range of <0.70 m, meaning that there was no additional emergence for about 1500 years after that event. Assuming older assemblages were not eroded, traces of emergence events older than 3000 years have not been found above the highest assemblage. These results suggest that this area began experiencing a RSL fall around 3000 years ago, with the falls becoming more frequent and larger in magnitude starting around 1500 years ago.

The lack of evidence of uplift prior to 3000 years ago in the study area is supported by an analysis of drilling core samples obtained from the Holocene lowland of central Ito City. The uppermost level of transgressive marine deposits, indicating an RSL rise subsequent to the Last Glacial Stage, is dated to around 4000 years ago and distributed at almost 0 m T.P. (Taguchi, 1993). Fujiwara et al. (2014) proposed that the RSL peaked at 3–4 m T.P. around 6800 years ago (Fig. 6). Although their estimation has an error of several meters, this means that there is no clear evidence of uplift at least higher than Zone 0.

5.2. Causes of emergence events

In considering the cause of emergence events, we discuss the effect of eustatic sea level change around the study area (Fig. 6). Geologically reconstructed Holocene sea level change in the Lake Inba area, which is an almost tectonically stable region near Tokyo, indicates that it may have been as low as −2 m below present sea level 3000 years ago (Chiba et al., 2016). However, no precise reconstruction has been proposed for the period from 1500 years ago. Okuno et al. (2014) simulated two theoretical RSL curves based on the glacial isostatic adjustment models with tide gauge observation data for each station in Japan. The simulation results for Ito indicate that the sea level was almost constant or gradually decreased by about 1 m over the past 4000 years. The intermittent RSL falls observed in the study area that occurred at 400- to 800-year intervals over the past 1500 years cannot be explained by such gradual sea level change on a millennial time scale, and thus were likely the result of crustal uplift caused by seismic activity, volcanic activity, or other tectonic processes. Although small fluctuations over the past 2000 years within 0.5 m of the eustatic sea level change such as those simulated by Grinsted et al. (2009) could possibly partially contribute to the RSL fall, here we mainly discuss the cause of the RSL reduction events in this area in relation to tectonic processes.

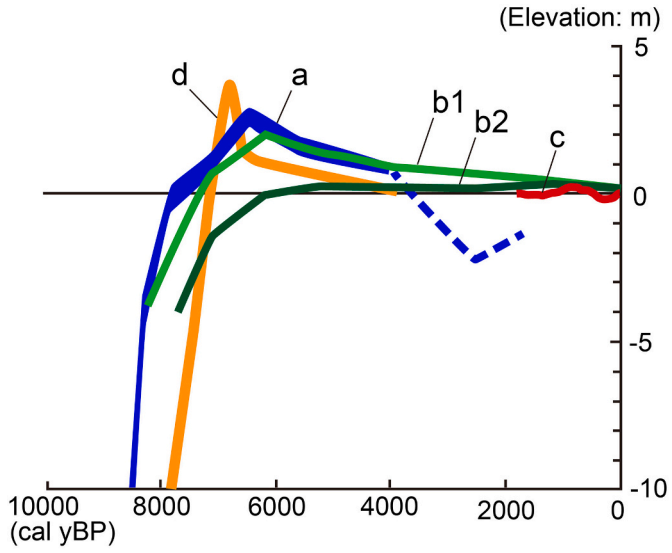

Fig. 6. Holocene sea level curves around the study area. a: Geologically reconstructed sea level curve in the Lake Inba area (calibrated with long term crustal movement) (Chiba et al., 2016). b1 and b2: Theoretically predicted RSL curve for Ito using ANU ice model (b1) and revised ANU ice model (b2) (Okuno et al., 2014). c: Theoretically predicted RSL curve for past 2000 years (Grinsted et al., 2009). d: Geologically reconstructed sea level change curve for Ito (not considered with crustal movement) (Fujiwara et al., 2014).

The difference in elevation between the upper limit of Zone 1 (3.50 m T.P.) and that of the present-day Pk assemblages (0.20 m T.P.) is approximately 3.30 m. Dividing this value by 1500 years yields a mean uplift rate of 2.20 mm/yr, which is extremely rapid compared with the mean apparent uplift rate range of 0.01 ± 0.01 to 1.47 ± 0.08 mm/yr obtained from the global database of uplifted coasts (Pedoja et al., 2014), but is often observed in volcanic areas (e.g. 1.7 mm/yr in Nisyros volcano; Stiros et al., 2005). Menant et al. (2020) simulated a million-year-scale forearc topographic signal caused by transient slab-top stripping events at the base of the forearc crust, suggesting that a related background uplift of 1–5 mm/year may affect the 10^1- to 10^3-year-scale crustal deformation covered in this study. However, since the study area is not located in the forearc region, but on a northern tip of a colliding volcanic arc, such a forearc deformation model cannot be directly applied.

Regarding the uplift process for each emergence event, we first examine crustal activity on the Izu Peninsula and surrounding areas based on instrument measurement data collected over the past 100 years or so and then verify the relationship between this activity and the emergence of Zone 3, which is dated to after 1830 CE. Based on the results of this examination, we discuss the relationship between the emergence of Zones 1 and 2 and seismic/volcanic activity known to have occurred based on historical and geological records. The cause of the emergence of Zone 0 and comprehensive tectonics in the late Holocene are discussed in Section 5.3.

5.2.1. Geodetically detected vertical crustal movement

A leveling survey was started in 1904 along a benchmark route running approximately 2 km west of the study area. The results of this survey can be discussed in relation to seismic and volcanic activities (Fig. 7). The 1923 Taisho Kanto earthquake, an interplate megathrust earthquake along the Sagami Trough, is one of the largest earthquakes in the vicinity of the study area. This earthquake was accompanied by up to ~2 m of coastal uplift of Sagami Bay and Boso Peninsula, but no major vertical crustal movement in the study area was observed (Figs. 1, 7) (Land Survey Department, 1926). Hatsushima Island, 9 km northeast of Ito, also uplifted ~1 m despite it being located on the foot wall side of the megathrust ruptured during the 1923 earthquake. Ishibashi (1988, b; 2004) proposed that the uplift of Hatsushima was caused by the West Sagami Bay Fracture (WSBF), which is a theoretically inferred offshore left-lateral reverse active fault striking in the N-S direction 5–10 km east of the study area (Fig. 1).

After the 1923 event, earthquake swarms occurred in the eastern part of the Izu Peninsula from February to April and in May 1930. These were followed by an inland shallow earthquake (M7.3) in November 1930 caused by the activity of the KIFZ (F1 in Fig. 5). To examine these events, a detailed leveling survey was repeatedly conducted between 1930 and 1933 by Tsuboi (1933). An analysis of these data indicates that the cumulative uplift along the leveling route reached approximately 0.30 m in this period; nevertheless, the deformation at the time of the M7.3 earthquake was at most on the order of 0.03 m. This phenomenon can be explained by the magma dike intrusion model (Nishimura and Murakami, 2007). The various tectonic events that have occurred in the vicinity of the study area in a short period are likely to be related to each other.

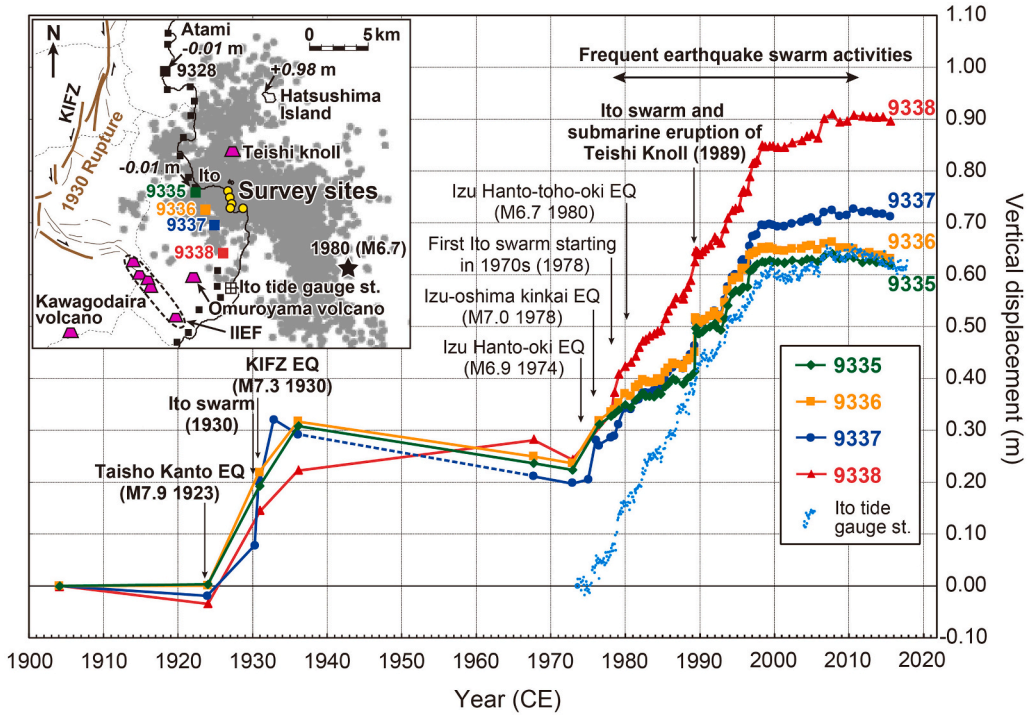

Fig. 7. Temporal change of vertical displacement at leveling benchmarks around Ito City (modified from Geospatial Information Authority of Japan, 2016) and inferred vertical displacement from tide gauge data from the Ito tide station (Coastal Movements Data Center, 2018). EQ: earthquake. Epicenters of major earthquakes are shown in Fig. 1 and inset. Vertical displacement of benchmarks is plotted relative to benchmark 9328. Tide gauge data show monthly levels relative to the level in July 1973. Inset shows location map of leveling benchmarks, surrounding seismic activity, volcanos, and active faults. The colored squares are the locations of graphed benchmarks. The large black square is the reference benchmark. The small black squares are the locations of other benchmarks. The gray dots in the background are epicenters of earthquake swarms during 1974–2011 (Japan Meteorological Agency, 2014). The star is the epicenter of the 1980 Izu Hanto-toho-oki earthquake. The fault trace for KIFZ is from the active fault database of Japan (https://gbank.gsj.jp/activefault/index). The purple trapezoids are volcanos that erupted during the late Holocene. Italic numbers are vertical crustal displacement during the 1923 Taisho Kanto earthquake (Land Survey Department, 1926).

The land level gradually subsided by about 0.10 m over the next 40 years but began to uplift again starting in 1974. Gradual uplift continued for approximately the next 24 years (until 1998), resulting in a cumulative uplift of 0.40 to 0.50 m (Fig. 7) (Geospatial Information Authority of Japan, 2016). Tide gauge data from Ito station since 1974 indicate the same trend as that for the benchmark leveling data. During this period, intermittent earthquake swarms and the 1989 Teishi Knoll eruption occurred (Japan Meteorological Agency, 2014). It has been reported that the crustal deformation during this period was caused by magmatic dyke intrusions, which resulted in episodic uplift whenever earthquake swarms occurred (e.g., Tada and Hashimoto, 1991; Okada and Yamamoto, 1991; Aoki et al., 1999). No significant change in deformation has been observed since the 2000s; the total amount of net uplift in approximately the past 100 years from the benchmark data is 0.60 to 0.70 m. This amount is the relative displacement with respect to benchmark 9328 in Atami, but since it is mostly consistent with the tide gauge data from Ito station, it can be correlated with the RSL change.

5.2.2. *Cause of emergence of Zone 3*

The geodetically detected uplifts during 1930–1933 and 1974–1998 coincide with the timing of the coastal emergence of Zone 3. No distinct coseismic vertical displacement in this period has been observed. Accordingly, the data indicates that the emergence of Zone 3 is associated with a volcanotectonic uplift due to subsurface magma movement. The total amount of RSL fall for Zone 3 is 0.82 m, which is slightly greater than the cumulative uplift of 0.60–0.70 m observed over the past 100 years. Considering that the leveling route is located approximately 2 km from the coast, one reason for this discrepancy may be spatial variability in the crustal deformation. Alternatively, because the oldest age estimated for Zone 3 is the mid-1800s, there is a possibility that another uplift event occurred prior to 1930. Historical documents indicate a record of earthquake swarms in 1816–1817 and 1868 or 1870 before the start of instrument measurements (Koyama, 1999; Table S1). The latter event falls within the age range of Zone 3. These findings suggest that Zone 3 emerged as a result of volcanotectonic uplift events in two steps around 1930–33 (~0.3 m) and 1974–1998 (~0.4–0.5 m), and possibly a third step around 1868–1870 (~0.1–0.2 m; assuming no subsidence during the period of 1870–1930). Based on the individual age data, the assemblages in the middle and upper sections of Zone 3 at Locs. 2 and 4 may be associated with the uplifts in 1868 or 1870 and 1930, and the assemblages in the lower section of Zone 3 at Loc. 2, which also included samples considered to be modern, may be associated with the uplift from 1974 to 1998.

5.2.3. *Cause of emergence of Zone 2*

As discussed in Section 5.1, Zone 2 can be vertically divided into two sections, which possibly emerged in a stepwise process over 100–200 years. This emergence process is similar to that in Zone 3, whose causes can thus be applied to Zone 2. Specifically, the distribution and age characteristics of Zone 2 can be explained if we assume that two separate uplift events resulting from subsurface magma movement occurred in two periods (1356–1470 and 1482–1666 CE) within 100–200 years. Regarding the latter period, the possibility of an earthquake swarm event in 1596 has been proposed based on historical records (Koyama, 1999; Table S1). The historical records describe frequent earthquakes for a month, although Koyama (1999) proposed that it may have been aftershocks caused by another seismic source event around the Izu area. No other historical records of localized events such as small eruptions or earthquake swarms suggesting magma intrusion have been found (note that historical records in Japan are scarce before the 16th century). It is thus necessary to consider other possible causes.

Although the records of large earthquakes are incomplete for this period, the vicinity of the study area experienced interplate megathrust earthquakes probably in 1293 and possibly in 1433 or 1495 along the Sagami Trough (Ishibashi, 2020). As in the 1923 earthquake, for which no coastal uplift was observed in the study area, there are no historical

records regarding uplift in or around Ito associated with these earthquakes. However, as in the 20th century, interplate megathrust earthquakes along the Sagami Trough could have triggered a period of volcanic and seismic activity around the study area in the following century. Alternatively, it is possible that the offshore intraplate faults in the western Sagami Bay may have simultaneously ruptured, producing uplift in the study area.

The WSBF is one such candidate offshore fault despite the fact that it caused no uplift during the 1923 earthquake in the study area (Fig. 1). Okamura et al. (1999) identified a reverse fault several kilometers east of the inferred line of the WSBF based on an interpretation of the offshore seismic profiles. Multiple levels of Holocene marine terraces below ~10 m T.P. can be identified on Hatsushima Island, indicating that the WSBF may have repeatedly ruptured. Radiocarbon ages indicate that the Holocene uppermost terrace formed 6000–7000 years ago, but the other lower terraces have not yet been dated (Ishibashi et al., 1982). If a past rupture of the WSBF extended southward, it would contribute to coastal emergence in the study area. To examine the uplift due to the activity of the WSBF, we thus calculated vertical crustal deformation using a fault model (Okada, 1985) (Fig. 8; Table 2). Our proposed fault is established with a length of 40 km along the assumed trace of the WSBF. The northern end of the fault is delimited by the coastline because the inland fault trace cannot be geomorphologically identified, and the southern end is determined by referring to the distribution of the submarine scarp. The fault dip and rake are set to 80° and 60°, respectively, according to Ishibashi (1988, 2004) and Aida (1993). The fault width is determined to be 10 km referring to the depth distribution of the seismogenic layer in this area (Headquarters for Earthquake Research Promotion, Earthquake Research Committee, 2015). The slip amount is set to 4 m using the relationship between the length and the slip amount of the active fault reported by Matsuda (1975). This fault can produce about 0.4 m of uplift in the study area and its activity may partially contribute to the emergence of Zone 2. However, it is unlikely that such faulting events would repeat a few times with short recurrence intervals only during this period to explain the entire emergence.

Offshore active faults have also been identified off Shimoda, the southernmost part of the Izu Peninsula (Fig. 1). Kitamura et al. (2015) proposed two fault models that can explain the distribution of uplift reconstructed from emerged sessile assemblages over the past 3000

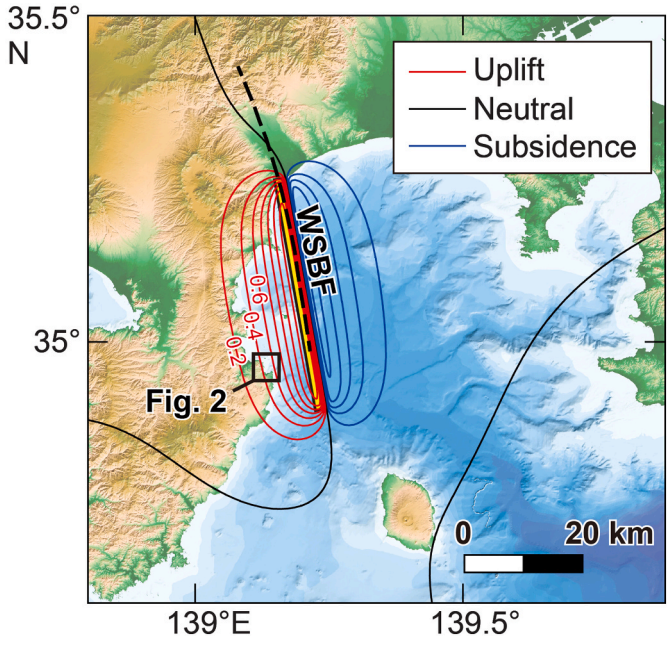

Fig. 8. Vertical crustal movement simulated from a fault model along the Western Sagami Bay Fault. Contour interval is 0.2 m.

Table 2
Parameters for fault model of WSBF.

Latitude (deg N)*	35.25295
Longitude (deg E)*	139.16784
Depth (km)*	1
Length (km)	40
Width (km)	10
Strike angle (deg)	170
Dip angle (deg)	80
Rake angle (deg)	60
Slip amount (m)	4
Moment magnitude**	7.1

* Latitude, longitude, and depth refer to the northeastern corner of the fault plane.
** A rigidity of 4×10^{10} N/m^2 is assumed.

years around the tip of the peninsula. The proposed younger two uplift events are dated to 1430–1660 and 1506–1815 CE (mean uplift 1.1–1.5 m each), which seem to coincide with the timing of the two emergence events for Zone 2. However, it is unreasonable to assume that these sets of events are correlated because the proposed source faults are too far away to cause uplift in the study area. If these events are correlated, they would correspond to a very large-wavelength uplift, suggesting volcanotectonic emergence rather than coseismic fault displacement.

An inland faulting event in this period caused by the KIFZ has been detected based on trenching survey data (Kondo et al., 2003). The timing of the F2 event, recalibrated using the IntCal 20 curve (Reimer et al., 2020), is estimated to be between 1320 and 1420 CE, which roughly coincides with the estimated emergence period of Zone 2 (Fig. 5). Given that the coseismic uplift caused by fault activity in 1930 was quite small (0.03 m) along the leveling route due mainly to strike slip, and that no inland fault traces have been identified around the study area, it is unlikely that KIFZ activity was directly involved in the emergence of Zone 2. Considering that the earthquake swarm event in 1930 was probably correlated with the 1930 faulting event of KIFZ, an earthquake swarm synchronized with the F2 event may have occurred, causing uplift for the same reason as the emergence of Zone 3.

If no tectonic movement occurred in the period from the upper to lower sections, another possible cause of emergence due to an RSL fall of at least 0.30 m (as estimated from the vertical span of Zone 2) is regional or eustatic sea level change. The time difference between the inferred event ages of the two sections is 310 years at maximum. This interval implies that the RSL fell at a rate of about 0.1 m/100 years, which can be explained by eustatic sea level change (e.g., sea level curve c in Fig. 6 simulated by Grinsted et al., 2009). Similar aseismic phenomena of almost the same age have been proposed for two sites along the coast of the Sea of Japan (Fig. 1): a 0.30–0.40 m RSL fall in 1430–1655 CE or later in the Noto Peninsula (Shishikura et al., 2009), and a 0.40 m RSL fall in 1342–1418 CE or later in Hamada (Shishikura et al., 2020). However, in these reports, eustatic sea level change is just one hypothesis among several interpretations to explain the observed emerged shoreline features.

In summary, the cause of the emergence of Zone 2 can be attributed to either volcanic uplift, coseismic uplift due to the activity of an offshore fault, or a combination of these uplifts with a eustatic sea level fall. Referring to the emergence process for Zone 3 as a modern analog, volcanic uplift is the most likely. As in the case of the earthquake swarm event in 1930, which occurred in close proximity to large earthquakes in 1923 and 1930, the emergence of each zone may have occurred during a period of tectonic activity in and around the study area. The volcanic uplift due to subsurface magma movement for the emergence of Zone 2 may also be related to historical interplate megathrust earthquakes and KIFZ activity in the period of Zone 2 (Fig. 5).

5.2.4. *Cause of emergence of Zone 1*

Considering the tectonic setting of the study area, it is highly likely that the emergence of Zone 1 was also caused by uplift associated with

subsurface magma movement. However, based on the distribution of ^{14}C sample elevations and ages, the entire zone appears to have emerged via a single event and may not have undergone the stepwise emergence process hypothesized for Zones 2 and 3. If the emergence of Zone 1 was caused by a single event, that event may have been coseismic uplift. No descriptions of earthquakes in the inferred emergence period of Zone 1 (595–715 CE) have been found (note that there are very few historical records from this period). Nevertheless, within the ^{14}C age range for Zone 1, large earthquakes that caused damage in and around the Izu Peninsula in 841 and 878 have been identified (Usami et al., 2013). The 841 event was correlated with the activity of the KIFZ based on the results of a trenching survey (F3 in Fig. 5) (Kondo et al., 2003). The 878 event was interpreted as an interplate megathrust earthquake along the Sagami Trough based on historical documents (Ishibashi, 2020). If the marine reservoir effect of a positive ΔR value, such as +109 yr for Shimoda (Yoneda et al., 2000), is applied, the 841 and 878 events move closer to the inferred emergence period for Zone 1. As discussed in Section 5.2.2, it is unlikely that an interplate megathrust earthquake along the Sagami Trough and a faulting event of the KIFZ directly uplifted the study area. However, the concentration of such tectonic events over a period of 100–200 years is similar to the situation for Zones 2 and 3, suggesting that tectonic and magmatic activities in the surrounding area induced the uplift of Zone 1.

5.3. Late Holocene tectonics in Higashi-Izu monogenetic volcano field

5.3.1. Crustal uplift over past 3000 years

Zone 0 which is the oldest and has the highest elevation in the study area, was observed at Loc. 2. Although the cause of the emergence of the assemblage is difficult to identify due to the limited distribution, the emergence is dated to 1265–926 BCE, which coincides with the timing of the Kawagodaira eruption (the largest eruption of the Higashi-Izu monogenetic volcano group during the last 100,000 years), estimated to be 1210–1187 BCE (Tani et al., 2013). Thus, it appears that the initiation of intermittent emergence events in the study area coincides with the start of Holocene volcanic activity in the Higashi-Izu monogenetic volcano field. Such simultaneity is also observed in the southern part of the peninsula. The uppermost level of emerged sessile assemblages (2.7–3.5 m T.P.) and post-glacial transgressive deposits (1.2–1.4 m T.P.) are dated to around 3000 years ago (Taguchi, 1993; Kitamura et al., 2014, 2015), with no evidence of uplift prior to this.

These results suggest that crustal uplift in the Izu Peninsula began around the time of the Kawagodaira eruption about 3000 years ago. This is probably closely related to the magma formation process for the Higashi-Izu monogenetic volcano group. This group produced a total magma discharge of 5.5 billion tons over 150,000 years. Its first 50,000 years saw two eruptions with a discharge of 0.6 to 1 billion tons, but it remained inactive for the following 60,000 years, with only a few minor eruptions. The volcano group became slightly more active around 40,000 years ago, but the most active period was the last 4000 years, with three large eruptions, the Omuroyama (510 million tons), Kawagodaira (760 million tons), and Iwanoyama-Ioyama (360 million tons) eruptions, occurring in short succession. The average magma discharge rate has increased since 40,000 years ago, and has been particularly high since 4000 years ago (Koyama et al., 1995). While the initial eruptions after 150,000 years ago discharged only basaltic magma, eruptions of andesitic magma began to occur after 15,000 years ago, and the Omuroyama eruption 4000 years ago also discharged andesitic magma. However, the subsequent Kawagodaira eruption about 3000 years ago was the first dacitic-rhyolitic eruption in the Higashi-Izu monogenetic volcano group. The subsequent Iwanoyama-Ioyama eruption also discharged andesitic and dacitic-rhyolitic magma (Koyama et al., 1995). The formation of andesitic to rhyolitic magma is thought to be caused by melting of the upper crust due to a rise in temperature around the upper/lower crustal boundary (Koyama and Umino, 1991). The generation of large amounts of andesitic to rhyolitic magma in the crust may have given buoyancy to the upper crust and caused the widespread uplift of the Izu Peninsula starting around 3000 years ago and the emergence of Zone 0.

5.3.2. Relationship between the emergence events and surrounding volcanic and seismic activity

In the period from 3000 to 1500 years ago, the amount of uplift appears to be negligible in comparison to uplift from 1500 years ago to present. This may indicate volcanotectonic process related to the change of magmatic activity in this area. However, referring to the RSL curve proposed by Chiba et al. (2016), it is possible that the sea level around 3000 years ago was 2 m lower than the present day, and then began to rise (Fig. 6). If such a sea level rise occurred, it may have played a role in offsetting the uplift, resulting in a seemingly slower uplift rate. In this case, intermittent uplift with intervals of 400–800 years may have occurred not only in the past 1500 years but also in the period from 3000 to 1500 years ago.

For the past 1500 years, at least three emergence events have occurred at intervals of 400–800 years in the study area. During this period, no significant volcanic eruptions occurred except for a small eruption of the Teishi Knoll in 1989 (Fig. 5). As observed in recent events related to the emergence of Zone 3, volcanic uplift due to magma intrusion events without significant volcanic eruptions is one of the major characteristics of the Higashi-Izu monogenetic volcano field (Koyama et al., 1995). Subsurface magma movement generally can only be detected in areas where modern instrumental observation networks are well established, and it is quite difficult to evaluate long-term activity over historical and pre-historical periods. However, by combining instrumental observation data in the last 100 years and geological data for emerged shoreline features, it can be proposed that magma intrusion events may have been periodically active on a scale of several hundred years. Surrounding seismic activity indicates that the KIFZ may have ruptured at intervals of 460 to 1600 years, and that interplate megathrust earthquakes along the Sagami Trough may have occurred at a mean recurrence interval of about 400 years, and their timing almost overlaps with emergence events (Fig. 5). It is possible that magmatic activity is triggered by such earthquake cycles.

6. Conclusion

We investigated emerged shoreline features along the coast of Ito, the eastern part of Izu Peninsula, Japan to demonstrate the usefulness of uplift traces in the long-term and quantitative evaluation of subsurface magma movement and to verify their relationship to the surrounding tectonic setting. At least three levels of emerged shoreline features (Zones 1 to 3, in descending order) were identified in the study area. The RSL fall amounts (emergence dates) for the zones is inferred to be 1.05 m (595–715 CE), 1.33 m (1356–1666 CE), and 0.82 m (1830 CE or later), respectively, suggesting intermittent uplift in the past 1500 years with an interval of 400–800 years. Zone 3 emerged mainly due to recent vertical crustal movement caused by subsurface magmatic movement accompanied by earthquake swarms, which have geodetically caused gradual stepwise uplifts in 1930–1933 and 1974–1998. Including a possible uplift in 1868 or 1870 deduced from earthquake swarms in historical records, Zone 3 emerged over a period of 130 years. Zone 2 can be divided into upper and lower sections based on the age data, and, along with Zone 3, appears to have emerged via a stepwise process over a period of 100–200 years. This suggests that the cause of the emergence of Zone 2 is also volcanic uplift. However, because there is no historical evidence supporting earthquake swarms or volcanic eruptions around the study area, it is also possible that the emergence was also caused by coseismic uplift associated with the activity of offshore faults and/or a slight regional sea-level fall. The cause of the emergence of Zone 1 is also likely to be volcanic uplift, but coseismic uplift associated with the offshore faults should also be considered, as the sessile assemblage appears to have entirely emerged via a single event. Zone 0, the highest

assemblage overlying Zone 1, dated to about 3000 years ago, with no distinct evidence of earlier uplift. Its emergence coincides with the timing of the Kawagodaira eruption. Transgressive deposits in the Holocene lowland around the study area also indicate that the post-glacial highstand was 3000–4000 years ago. These facts suggest that the crustal uplift of the Izu Peninsula started around 3000 years ago due to Holocene volcanic activity, especially the largest eruption of the Kawagodaira volcano. For all emergence events of Zone 1 to 3, interplate megathrust earthquakes along the Sagami Trough, KIFZ activity, and magmatic activity occurred within a period of 100–200 years, suggesting that the crustal activities in and around the study area may have been correlated with each other to produce coastal uplift.

CRediT authorship contribution statement

Masanobu Shishikura: Methodology, Investigation, Data curation, Conceptualization, Project administration, Visualization, Writing – original draft. **Yuichi Namegaya:** Formal analysis, Investigation, Writing – review & editing. **Hiroyuki Kaneko:** Conceptualization, Investigation, Writing – review & editing. **Masato Koyama:** Writing – review & editing, Conceptualization, Investigation.

Declaration of Competing Interest

The authors declare that they have no known competing financial interests or personal relationships that could have appeared to influence the work reported in this paper.

Data availability

Data will be made available on request.

Acknowledgements

We appreciate Gino de Gelder and an anonymous reviewer for their constructive comments that have been helpful in improving the paper. This work was supported by the Geological Survey of Japan, National Institute of Advanced Industrial Science and Technology (AIST). Base maps in Figs. 1 and 8 were drawn using GMT (Wessel et al., 2013).

Appendix A. Supplementary data

Supplementary data to this article can be found online at https://doi.org/10.1016/j.tecto.2023.229985.

References

Acocella, V., 2021. Volcano-tectonic processes. In: Advances in Volcanology. Springer-Nature, Heidelberg.

Aida, I., 1993. Historical tsunamis and their numerical models which occurred in the North-Western part of Sagami bay. J. Geogr. (Chigaku-Zasshi) 102, 427–436 (in Japanese with English abstract).

Antonioli, F., Kershaw, S., Renda, P., Rust, D., Belluomini, G., Cerasoli, M., Radtke, U., Silenzi, S., 2006. Elevation of the last interglacial highstand in Sicily (Italy): a benchmark of coastal tectonics. Quat. Int. 145–146, 3–18. https://doi.org/10.1016/j.quaint.2005.07.002.

Aoki, Y., Segall, P., Kato, T., Cervelli, P., Shimada, S., 1999. Imaging magma transport during the 1997 seismic swarm off the Izu Peninsula, Japan. Science 286 (5441), 927–930.

Aramaki, S., Hamuro, K., 1977. Geology of the Higashi-Izu monogenetic volcanic group. Bull. Earthq. Res. Inst., Univ. Tokyo 52, 235–278 (in Japanese with English abstract).

Bird, P., 2003. An updated digital model of plate boundaries. Geochem. Geophys. Geosyst. 4 https://doi.org/10.1029/2001GC000252.

Bronk Ramsey, C., 2009. Bayesian analysis of radiocarbon dates. Radiocarbon 51, 337–360. https://doi.org/10.1017/S0033822200033865.

Catalano, S., Torrisi, S., Ferlito, C., 2004. The relationship between late Quaternary deformation and volcanism of Mt. Etna (eastern Sicily): new evidence from the sedimentary substratum in the Catania region. J. Volcanol. Geotherm. Res. 132, 311–334. https://doi.org/10.1016/S0377-0273(03)00433-5.

Chiba, T., Sugihara, S., Matsushima, Y., Arai, Y., Endo, K., 2016. Reconstruction of Holocene relative sea-level change and residual uplift in the Lake Inba area, Japan. Palaeogeogr. Palaeoclimatol. Palaeoecol. 441, 982–996. https://doi.org/10.1016/j.palaeo.2015.10.042.

Coastal Movements Data Center, 2018. Vertical Displacement of each Tide Station Using Analytical Method of Kato and Tsumura (1979). Coastal Movements Data Center, Tsukuba available from https://cais.gsi.go.jp/cmdc/center/katoutsumura2018.pdf (in Japanese).

Costa, A., Di Vito, M.A., Ricciardi, G.P., Smith, V.C., Talamo, P., 2022. The long and intertwined record of humans and the Campi Flegrei volcano (Italy). Bull. Volcanol. 84, 5 (2022). https://doi.org/10.1007/s00445-021-01503-x (2022).

Di Stefano, A., Branca, S., 2002. Long-term uplift rate of the Etna volcano basement (southern Italy) based on biochronological data from Pleistocene sediments. Terra Nova 14 (1), 61–68. https://doi.org/10.1046/j.1365-3121.2002.00389.x.

Firth, C., Stewart, I., Mcguire, W.J., Kershaw, S., Vita-Finzi, C., 1996. Coastal elevation changes in eastern Sicily: Implications for volcano instability at Mount Etna. Geol. Soc. Lond. Spec. Publ. 110, 153–167.

Fujiwara, O., Irizuki, T., Obayashi, I., Hirakawa, K., Hasegawa, S., Uchida, J., Abe, K., 2014. Relative sea-level change during 6,300–2,000 BC reconstructed from drilling cores from Ito City, eastern coast of the Izu Peninsula, central Japan. Quat. Res. (Daiyonki-Kenkyu) 53, 35–53 (in Japanese with English abstract).

Fukutomi, K., 1935. Crustal movements of Izu Peninsula, Central Japan, based on historical documents and oral traditions (part 1). J. Seismol. Soc. Japan (Zishin) Zisin, First Series 7, 145–153 (in Japanese).

Geospatial Information Authority of Japan, 2016. Crustal movements in the Izu peninsula and its vicinity. Rep. Coordinat. Committee Earthq. Predict. 96, 144–163 (in Japanese).

Grinsted, A., Moore, J.C., Jevrejeva, S., 2009. Reconstructing Sea level from paleo and projected temperatures 200 to 2100 AD. Clim. Dyn. https://doi.org/10.1007/s00382-008-0507-2.

Gudmundsson, A., 2020. Volcanotectonics. In: Understanding the Structure, Deformation and Dynamics of Volcanoes. Cambridge University Press. https://doi.org/10.1017/9781139176217.

Hayakawa, Y., Koyama, M., 1992. Eruptive history of the Higashi Izu monogenetic volcano field 1: 0–32ka. Bull. Volcanol. Soc. Japan 37, 167–181 (in Japanese with English abstract).

Headquarters for Earthquake Research Promotion, Earthquake Research Committee, 2015. Regional Evaluations of Active Faults in the Kanto Region: First Edition. https://www.jishin.go.jp/evaluation/long_term_evaluation/regional_evaluation/kanto-detail/ (in Japanese).

Heaton, T., Köhler, P., Butzin, M., Bard, E., Reimer, R., Austin, W., Bronk Ramsey, C., Grootes, P., Hughen, K., Kromer, B., Reimer, P., Adkins, J., Burke, A., Cook, M., Olsen, J., Skinner, L., 2020. Marine20 - the marine radiocarbon age calibration curve (0–55,000 cal BP). Radiocarbon 62, 779–820. https://doi.org/10.1017/RDC.2020.68.

Ishibashi, K., 1988. "Kanagawa-ken Seibu earthquake" and earthquake prediction I, II. Kagaku 58, 537–547, 771–780 (in Japanese).

Ishibashi, K., 2004. Seismotectonic modeling of the repeating M 7-class disastrous Odawara earthquake in the Izu collision zone, Central Japan. Earth Planets Space 56, 843–858.

Ishibashi, K., 2020. Ancient and medieval events and recurrence interval of great Kanto Earthquakes along the Sagami Trough, Central Japan, as Inferred from historiographical seismology. Seismol. Res. Lett. 91, 2579–2589. https://doi.org/10.1785/0220200073.

Ishibashi, K., Ota, Y., Matsuda, T., 1982. Holocene marine terraces and vertical crustal movement of Hatsu-shima Island in Sagami Bay Central Japan. J. Seismol. Soc. Japan (Zishin) 35, 195–212 (in Japanese with English abstract).

Japan Meteorological Agency, 2014. List of Earthquake Swarm Activity in the Higashi-Izu Monogenetic Volcanic Group available from https://www.data.jma.go.jp/svd/vois/data/tokyo/316_Izu-TobuVG/316_eq_swarm.html (in Japanese).

Kaizuka, S., 1992. Coastal evolution at a rapidly uplifting volcanic island; Iwo-Jima, western Pacific Ocean. Quat. Int. 15 (16), 7–16.

Kaneko, H., 2012. Tsunami deposits detected at Usami archeological site and re-evaluation of the earthquake and tsunami in the 4th year of Meio. Res. Ito City Hist. 10, 102–124 (in Japanese).

Kayanne, H., Yamamuro, M., Matsumoto, E., 1987. *Pomatoleios kraussi* (BAIRD) as a paleo sea level indicator on the southeast coast of Boso Peninsula, Central Japan. Quat. Res. (Daiyonki-Kenkyu) 26, 47–57 (in Japanese with English abstract).

Kelsey, H.M., 2015. Geomorphological indicators of past sea levels. In: Shennan, I., Long, A.J., Horton, B.P. (Eds.), Hand-Book of Sea Level Research. Wiley, Hoboken, pp. 66–82. https://doi.org/10.1002/9781118452547.ch5.

Kitamura, A., Koyama, M., Itasaka, K., Miyairi, Y., Mori, H., 2014. Abrupt late Holocene uplifts of the southern Izu Peninsula, Central Japan: evidence from emerged marine sessile assemblages. Island Arc 23, 51–61. https://doi.org/10.1111/iar.12059.

Kitamura, A., Mitsui, Y., Ishibashi, H., Kawate, S., Kim, H., 2015. Examination of an active submarine fault off the Southeast Izu Peninsula, Central Japan, using field evidence for coseismic uplift and a characteristic earthquake model. Earth Planets Space 67, 197. https://doi.org/10.1186/s40623-015-0367-z.

Komori, J., Shishikura, M., Ando, R., Yokoyama, Y., Miyairi, Y., 2017. History of the great Kanto earthquakes inferred from the ages of Holocene marine terraces revealed by a comprehensive drilling survey. Earth Planet. Sci. Lett. 471, 74–84. https://doi.org/10.1016/j.epsl.2017.04.044.

Komori, J., Shishikura, M., Ando, R., Yokoyama, Y., Miyairi, Y., 2021. A Bayesian approach to age estimation of marine terraces and implications for the history of the great Kanto earthquakes, Central Japan. Quat. Sci. Rev. 272 https://doi.org/10.1016/j.quascirev.2021.107217.

Kondo, H., Toda, S., Imaizumi, T., Tsutsumi, H., Sugishita, I., Nakata, T., Okumura, K., Shimazaki, K., Takada, K., Ikeda, T., Haraguchi, T., 2003. Recent non-characteristic

behavior along the Tanna Fault based on three-dimensional trenching and Geoslicer techniques. J. Seism. Soc. Japan 2nd ser. (Zisin) 55, 407–423 (in Japanese with English abstract).
Koyama, M., 1999. Pre-20th century of earthquake swarms and volcanic activity in the Higashi Izu monogenetic volcano field, based on historical documents. Quat. Res. (Daiyonki-Kenkyu) 38, 435–446 (in Japanese with English abstract).
Koyama, M., Umino, S., 1991. Why does the Higashi-Izu monogenetic volcano group exist in the Izu Peninsula? Relationships between late Quaternary volcanism and tectonics in the northern tip of the Izu-Bonin arc. J. Phys. Earth 39, 391–420.
Koyama, M., Hayakawa, Y., Arai, F., 1995. Eruptive history of the Higashi-Izu monogenetic volcano field 2: mainly on volcanoes older than 32,000 years ago. Bull. Volcanol. Soc. Japan (Kazan) 40, 191–209 (in Japanese with English abstract).
Land Survey Department, 1926. The change of elevation of land caused by the great earthquake of September 1st, 1923. Bull. Earthq. Res. Inst., Univ. Tokyo 1, 65–68 (in Japanese).
Marra, F., Florindo, F., Jicha, B.R., Nomade, S., Palladino, D.M., Pereira, A., Sottili, G., Tolomei, C., 2019. Volcano-tectonic deformation in the Monti Sabatini Volcanic District at the gates of Rome (Central Italy): evidence from new geochronologic constraints on the Tiber River MIS 5 terraces. Sci. Rep. 9, 11496. https://doi.org/10.1038/s41598-019-47585-8.
Marturano, A., Isaia, R., Aiello, G., Barra, D., 2018. Complex dome growth atCampi Flegrei caldera (Italy) in the last15 ka. J. Geophys. Res. Solid Earth 123, 8180–8197. https://doi.org/10.1029/2018JB015672.
Matsuda, T., 1975. Magnitude and Recurrence Interval of Earthquakes from a Fault, Japan. J. Seismol. Soc. Japan (Zishin) 28, 269–283 (in Japanese with English abstract).
Matsuda, T., 1978. Collision of the Izu-Bonin arc with Central Honshu: Cenozoic tectonics of the Fossa magna, Japan. J. Phys. Earth 26 (Suppl), S409–S421.
Menant, A., Angiboust, S., Gerya, T., Lacassin, R., Simoes, M., Grandin, R., 2020. Transient stripping of subducting slabs controls periodic forearc uplift. Nat. Commun. 11, 1823. https://doi.org/10.1038/s41467-020-15580-7.
Miyabe, N., 1931. On the vertical earth movements in Kwanto districts. Bull. Earthq. Res. Inst. Tokyo Univ. 9, 1–21.
Mori, K., 1986. Life history and its variation of an intertidal dal barnacle, *Chthamalus challengeri* Hoek (preliminary report). Benthos Res. 29, 50–57 (in Japanese with English abstract).
Nasu, N., Kishinouye, F., Kodaira, T., 1931. Recent seismic activities in the Idu peninsula (part 1.). Bull. Earthq. Res. Inst., Univ. Tokyo 9, 22–35.
Nelson, A.R., 2013. Sea-levels, late Quaternary, Tectonics and relative sea-level change A2—Elias, Scott A. In: Mock, C.J. (Ed.), Encyclopedia of Quaternary Science, second edition. Elsevier, Amsterdam, pp. 503–519. https://doi.org/10.1016/B978-0-444-53643-3.00141-2.
Nishimura, T., Murakami, M., 2007. Dike Intrusion Model of the 1930 off Ito Earthquake Swarm estimated from Leveling Data. Bull. Volcanol. Soc. Japan (Kazan) 52, 149–159 (in Japanese with English abstract).
Okada, Y., 1985. Surface deformation due to shear and tensile faults in a half-space. Bull. Seismol. Soc. Am. 75, 1135–1154.
Okada, Y., Yamamoto, E., 1991. Dyke intrusion model for the 1989 seismovolcanic activity off Ito, Central Japan. J. Geophys. Res. Solid Earth 96 (B6), 10361–10376.
Okamura, Y., Yuasa, M., Kuramoto, S., 1999. Geological map of Suruga Bay 1:200,000. In: Marine Geology Map Series 52. Geological Survey of Japan, Tsukuba (in Japanese with English captions).
Okuno, J., Nakada, M., Ishii, M., Miura, H., 2014. Vertical tectonic crustalmovements along the Japanese coastlines inferred from late Quaternary and recent relative sea-level changes. Quat. Sci. Rev. 91, 42–61. https://doi.org/10.1016/j.quascirev.2014.03.010.
Pedoja, K., Husson, L., Johnson, M.E., Melnick, D., Witt, C., Pochat, S., Nexer, M., Delcaillau, B., Pinegina, T., Poprawski, Y., Authemayou, C., Elliot, M., Regard, V., Garestier, F., 2014. Coastal staircase sequences reflecting sea-level oscillations and tectonic uplift during the Quaternary and Neogene. Earth Sci. Rev. 132, 13–38. https://doi.org/10.1016/j.earscirev.2014.01.007.
Pirazzoli, P.A., 1996. Sea-Level Changes; the Last 20,000 Years. Wiley, Chichester.
Reimer, P.J., Austin, W.E.N., Bard, E., Bayliss, A., Blackwell, P.G., Ramsey, C.B., Butzin, M., Cheng, H., Edwards, R.L., Friedrich, M., Grootes, P.M., Guilderson, T.P., Hajdas, I., Heaton, T.J., Hogg, A.G., Hughen, K.A., Kromer, B., Manning, S.W., Muscheler, R., Palmer, J.G., Pearson, C., van der Plicht, H., Reimer, R.W., Richards, D.A., Scott, E.M., Southon, J.R., Turney, C.S.M., Wacker, L., Adolphi, F., Büntgen, U., Capano, M., Fahrni, S., Fogtmann-Schulz, A., Friedrich, R., Köhler, P., Kudsk, S., Miyake, F., Olsen, J., Reinig, F., Sakamot, M., Sookdeo, A., Talamo, S., 2020. The IntCal20 Northern Hemisphere radiocarbon age calibration curve (0-55 kcal BP). Radiocarbon 62, 725–757. https://doi.org/10.1017/RDC.2020.41.
Research Group for Active Fault of Japan (Eds.), 1991. Active Faults in Japan Sheet Maps and Inventories. University of Tokyo Press, Tokyo, p. 437.
Ristuccia, G.M., Di Stefano, A., Gueli, A.M., Monaco, C., Stella, G., Troja, S.O., 2013. OSL chronology of Quaternary terraced deposits outcropping between Mt. Etna volcano and the Catania Plain (Sicily, southern Italy). Phys. Chem. Earth 63, 36–46. https://doi.org/10.1016/j.pce.2013.03.002.
Rovere, A., Raymo, M.E., Vacchi, M., Lorscheid, T., Stocchi, P., Gomez-Pujol, L., Harris, D.L., Casella, E., O'Leary, M.J., Hearty, P.J., 2016. The analysis of last Interglacial (MIS 5e) relative sea-level indicators: Reconstructing Sea-level in a warmer world. Earth Sci. Rev. 159, 404–427. https://doi.org/10.1016/j.earscirev.2016.06.006.
Rust, D., Kershaw, S., 2000. Holocene tectonic uplift patterns in northeastern Sicily: evidence from marine notches in coastal outcrops. Mar. Geol. 167, 105–126. https://doi.org/10.1016/S0025-3227(00)00019-0.
Shimazaki, K., Kim, H.Y., Chiba, T., Satake, K., 2011. Geological evidence of recurrent great Kanto earthquakes at the Miura Peninsula, Japan. J. Geophys. Res. 116 (B12408) https://doi.org/10.1029/2011JB008639.
Shishikura, M., 2003. Cycle of interplate earthquake along the Sagami trough, deduced from tectonic geomorphology. Bull. Earthq. Res. Inst., Univ. Tokyo 78, 245–254 (in Japanese with English abstract).
Shishikura, M., 2014. History of the paleo-earthquakes along the Sagami Trough, central Japan–Review of coastal paleoseismological studies in the Kanto region. Episodes 37, 246–257. https://doi.org/10.18814/epiiugs/2014/v37i4/004.
Shishikura, M., 2019. New outcrop data of sessile assemblages uplifted due to the Kanto earthquakes in the southwestern coast of the Boso Peninsula, Central Japan. Hist. Earthq. (Rekishi-Jishin) 34, 91–101 (in Japanese with English abstract).
Shishikura, M., Echigo, T., Kaneda, H., 2007. Marine reservoir correction for the Pacific coast of Central Japan using ^{14}C ages of marine mollusks uplifted during historical earthquakes. Quat. Res. 67, 286–291. https://doi.org/10.1016/j.yqres.2006.09.003.
Shishikura, M., Echigo, T., Namegaya, Y., 2009. Evidence for coseismic and aseismic uplift in the last 1000 years in the focal area of a shallow thrust earthquake on the Noto Peninsula, west-Central Japan. Geophys. Res. Lett. 36, L02307. https://doi.org/10.1029/2008GL036252.
Shishikura, M., Namegaya, Y., Maemoku, H., Echigo, T., 2020. Coseismic uplift of Iwami-Tatamigaura during the 1872 Hamada Earthquake–Survey of emerged sessile assemblage and topography. J. Seismol. Soc. Japan (Zishin) 73, 159–177 (in Japanese with English abstract).
Stiros, S.C., Pirazzoli, P.A., Fontugne, M., Arnold, M., Vougioukalakis, G., 2005. Late-Holocene coastal uplift in the Nisyros volcano (SE Aegean Sea): evidence for a new phase of slow intrusive activity. Develop. Volcanol. 7, 217–225. https://doi.org/10.1016/S1871-644X(05)80041-5.
Sugimura, A., 1972. Plate boundaries near Japan. Kagaku (Science) 42, 192–202 (in Japanese).
Tada, T., Hashimoto, M., 1991. Anomalous Crustal Deformation in the Northeastern Izu Peninsula and its Tectonic significance Tension Crack Model. J. Phys. Earth 39 (1), 197–218.
Taguchi, K., 1993. Holocene relative sea-level change in the Izu Peninsula, Central Japan. Quat. Res. (Daiyonki-Kenkyu) 32, 13–29 (in Japanese with English abstract).
Tani, S., Kitagawa, H., Wan, H., Park, J.H., Sung, K.S., Park, G., 2013. Age determination of the Kawagodaira volcanic eruption in Japan by ^{14}C wiggle-matching. Radiocarbon 55, 748–752. https://doi.org/10.1017/S0033822200057908.
The Tanna Fault Trenching Research Group, 1983. Trenching study for Tanna Fault, Izu, at Myoga, Shizuoka Prefecture, Japan. Bull. Earthq. Res. Inst., Univ. Tokyo 58, 797–830 (in Japanese with English abstract).
Todesco, M., Costa, A., Comastri, A., Colleoni, F., Spada, G., Quareni, F., 2013. Vertical ground displacement at Campi Flegrei (Italy) in the fifth century: Rapid subsidence driven by pore pressure drop. Geophys. Res. Lett. 41, 1471–1478. https://doi.org/10.1002/2013GL059083.
Tsuboi, C., 1933. Vertical crustal displacement in the seismic region of Ito, on the east coast at the Idu Peninsula. Bull. Earthq. Res. Inst., Univ. Tokyo 11, 488–499.
Usami, T., Ishi, H., Imamura, T., Takemura, M., Matsuura, R., 2013. Materials for Comprehensive List of Destructive Earthquakes in Japan 599–2012. Univ. Tokyo Press, Tokyo (in Japanese).
Wessel, P., Smith, W.H.F., Scharroo, R., Luis, J., Wobbe, F., 2013. Generic Mapping Tools: improved version released. EOS Trans. AGU 94, 409–410.
Yoneda, M., Kitagawa, H., van der Plicht, J., Uchida, M., Tanaka, A., Uehiro, T., Shibata, Y., Morita, M., Ohno, T., 2000. Pre-bomb marine reservoir ages in the western North Pacific: preliminary result on Kyoto University collection. Nucl. Inst. Methods Phys. Res. B 172, 377–381.